# Enabling Technologies for Robot Assisted Ultrasound Tomography

Computer Integrated Surgery II

**Group 11 - Project Report**

Team Members: Fereshteh Aalamifar, Rishabh Khurana

Mentors: Emad Boctor, Iulian Iordachita, Russell Taylor

May 2013

## Abstract

A robot assisted ultrasound imaging system is developed to enable a robot operated probe following another probe held by a technician. The two probes system can be used for soft tissue ultrasound tomography. It can also be used for faster ultrasound scanning or more depth ultrasound imaging for obese patients.

The main challenge is to have the two probes properly aligned. Three loops of tracking are proposed; two of them are implemented and a feasibility experiment is conducted for the third one.

Two ultrasound calibrations and one hand-eye calibrations enable the two loops of tracking. The system functionality is tested and evaluations are carried out on the accuracy of calibrations.

The system is designed in a way to provide a portable, compact, light-weight system. Except for the robot, other components can be easily relocated. The tracking system is incorporated such that its proper functionality at any setup is automatically ensured without the need to determine its workspace.

# 1 Table of Contents

# 2 Introduction

The Ultrasound penetration is 10-15 cm maximum. The deeper the tissue, the more attenuation is caused, and consequently, the less quality images can be obtained. This is why ultrasound cannot be used for thick tissues or obese patients. In addition since ultrasound waves cannot travel through air, ultrasound imaging has limitations to be used for tomography. In this project, we develop a system which is a combination of human operated probe and a probe attached to a robotic arm. This system can be used to offer higher imaging depth, and to enable ultrasound tomography imaging.

## *2.1 Statement of Relevance/Importance*

Ultrasound machine is inexpensive, has a light weight, and more importantly, does not produce ionizing radiation which is believed to be dangerous to human health. In addition, CT is mostly used for bony structures while ultrasound is used for soft organs. Table 1 compares ultrasound and CT.

These advantages are the reasons why when the ultrasound was introduced to medical imaging in mid-twentieth century [1], many people started to build ultrasound systems for tomography to create 3D diagnostic images [2]. However, since ultrasound waves do not travel in air, they had to ask the patient to lie in a pool of water and they rotated ultrasound probes around the patient. However, in these types of systems, firstly, it is difficult to lie in a pool of water for many patients; second, the ultrasound image quality is not as good as other modalities and its penetration is limited to around 10 cm; and third, the sonographer do not have enough control over the ultrasound probe to exactly determine the part to be imaged.

**Table 1. CT vs Ultrasound (Adapted from [3], [4], [5])**

| | CT | Ultrasound |
|---|---|---|
| **Cost of a scan procedure** | $1200-$3200 | $100-$1000 |
| **Imaged structure** | Bony structures | Soft or internal organs |
| **Radiation exposure** | 2-10 msv | None |
| **Weight** | 2000 kg (for a 1000 mm diameter x 5000 mm long scanner) | ≥ 5 Kg |
| **Scan time** | < 30 secs | 10-15 min |

Today with the help of advances in computer systems and medical imaging technologies, we have access to better quality ultrasound images and faster processors which can perform much more complex tasks in seconds. This has on one hand authorized us to combine imaging technologies and on the other hand emerged the need for inventing new systems benefiting from ultrasound imaging. In this project, we build a system which can be used for ultrasound tomography but does not require the use of the pool of water; can cover higher imaging depth; and in addition is directly controlled by sonographer.

In this project we develop a system which combines a human operated ultrasound probe with a robotic one. Figure 1 shows an example of such system to produce ultrasound images of patient's leg. The sonographer starts scanning the area to be diagnosed; and a robot tracks the sonographer hand, on the other side of the patient's body, in order to align the two probes. These two probes

can both contain their own transmitter and receiver (a normal probe), or one of them take the transmitter role and the other be the receiver. This system can be used to cover higher depth imaging, to produce ultrasound tomographic images, or for faster real-time scanning. However, the final future goal is to develop a prototype that can provide ultrasound images for ultrasound tomographic imaging of soft tissue.

**Figure 1. An example of a robot assisted ultrasound scanning**

## *2.2 Contributions*

In this project we deliver:

- ultrasound calibrated probes and hand-eye calibrated endeffector,
- a robot operated mock ultrasound probe following the position of a free hand ultrasound probe using tracking system combined with B-mode tracking,
- an experiment showing feasibility of Energy Profile Tracking (EPT), and
- evaluation study of calibrations.

## *2.3 Hardware and software tools*

The list of main hardware and software tools used in this project is as follows: 5 DOF Robodoc, two mock ultrasound probes, 60 mm 128 array ultrasound probe, ultrasound machines, MicronTracker, Matlab, Solidworks, and visual studio.

## *2.4 Project demos*

A demo of the project can be found in the following link:

http://www.youtube.com/watch?v=lEz-sdVK4X8

And the EPT experiment demo can be found at:

http://www.youtube.com/watch?v=z9_ahzlt0tI

## *2.5 Report's organization*

In the next section of this report, we will explain the technical approach including project schematics, mechanical designs, tracking system, robot and software, experiments and calibrations. In section 3, conclusion and future work are provided while section 4 explains our management plan summary. The report ends with acknowledgement, references, and appendix.

# 3 Technical Approach

The system components and schematics are shown in Figure 2. The system is divided into three main sets of components. On one side, the freehand probe is operated by the technician scanning one side of the tissue. This probe has a marker attached to it which can be tracked by the tracking system. The tracking system sends data through IEEE 1394 PCI card to the computer and to the tracker API. On the other side, the tracker's camera is rigidly attached to the robot endeffector and to the robot operated probe. The software interface integrates data from the tracker's API and robot-server, processes the position data and calculates the goal position using cisst/saw libraries, and sends appropriate commands to the robot.

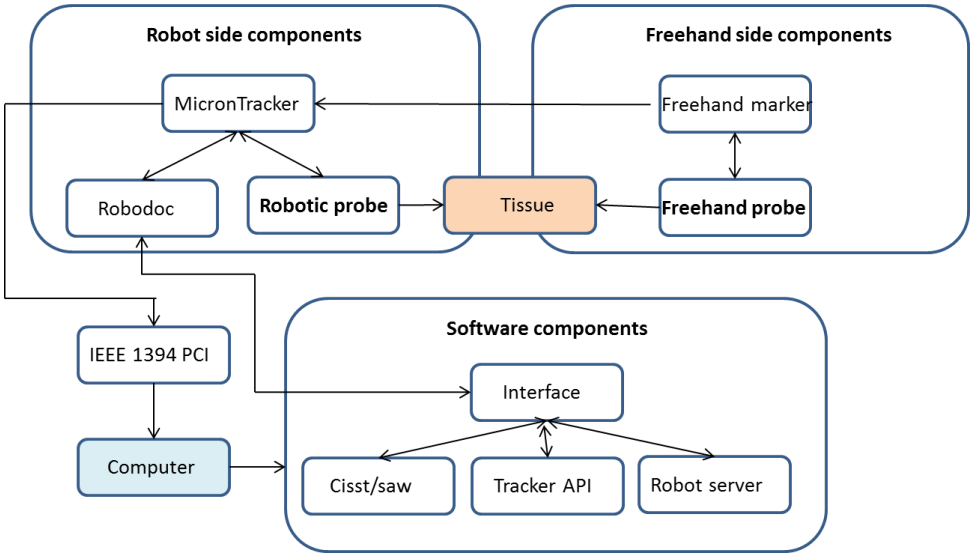


**Figure 2. System components and schematics**

## *3.1 Mechanical Designs*

In order to implement the system, firstly, we required several mechanical designs and manufacturing which are explained in the following sections.

### 3.1.1 Mock ultrasound probes

In the first phase, in order to reduce the system complication, two mock ultrasound probes mimicking shape and dimensions of a real ultrasound probe were designed in Solidworks and then manufactured using 3D printing machine. Figure 3 shows design and manufacturing of the mock probes.

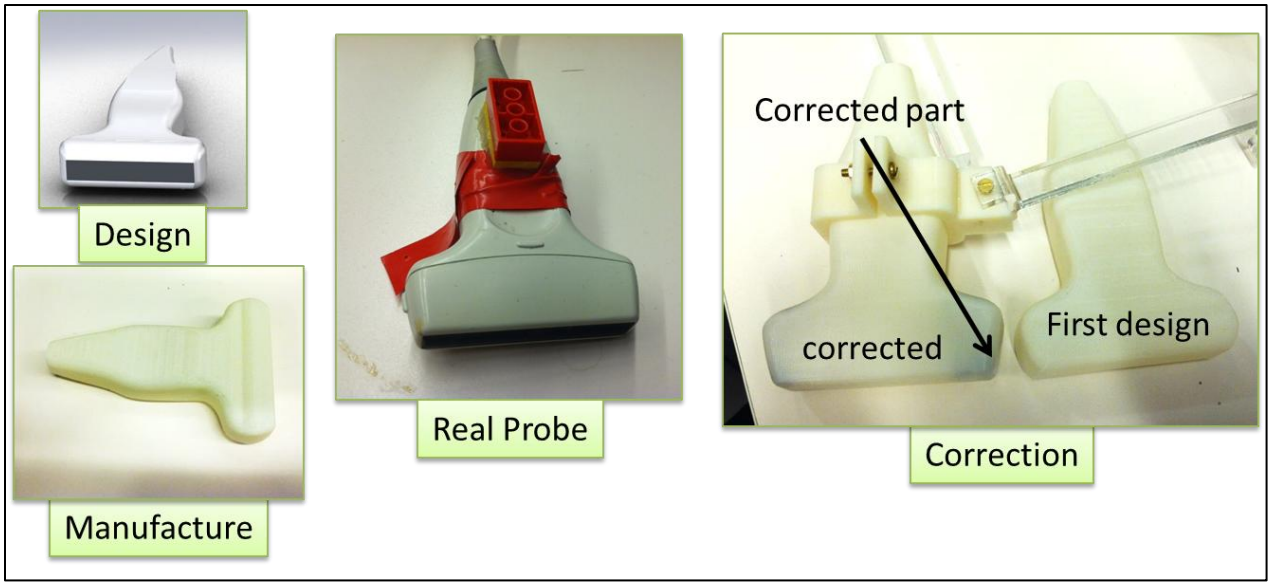


**Figure 3. Design and manufacturing of mock probes**

### 3.1.2 Freehand probe holder

In order to attach the tracker's marker to the freehand probe, a probe holder was designed and manufactured using laser cutter and 3D printing machines. Figure 5 shows the CAD design and picture of the freehand probe holder together with the corrections. Please refer to section 3.2.2 for explanation of the reason of such a design. The freehand probe holder consists of three components: ring, rod, and marker surface. The ring built using the 3D printer was not strong enough and could easily break. In order to reduce the force on the ring curves, we built the robot operated probe as two separate parts connected with two screws while the freehand ring (the more fragile one) has been built as one part with one screw.

When the freehand mock probe was replaced with a real ultrasound probe, due to a mismatch between the mock probe dimensions and the real one, we modified the freehand probe holder and used two side screws to have a stronger ring. In addition, instead of 3D printing, we used laser cutter and 5'' acrylic material to have a more rigid ring. The real probe's marker holder and ring are shown in Figure 4.

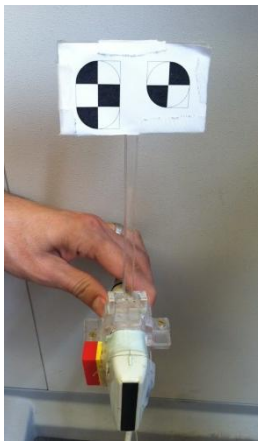

**Figure 4. Freehand ultrasound probe holder and ring**

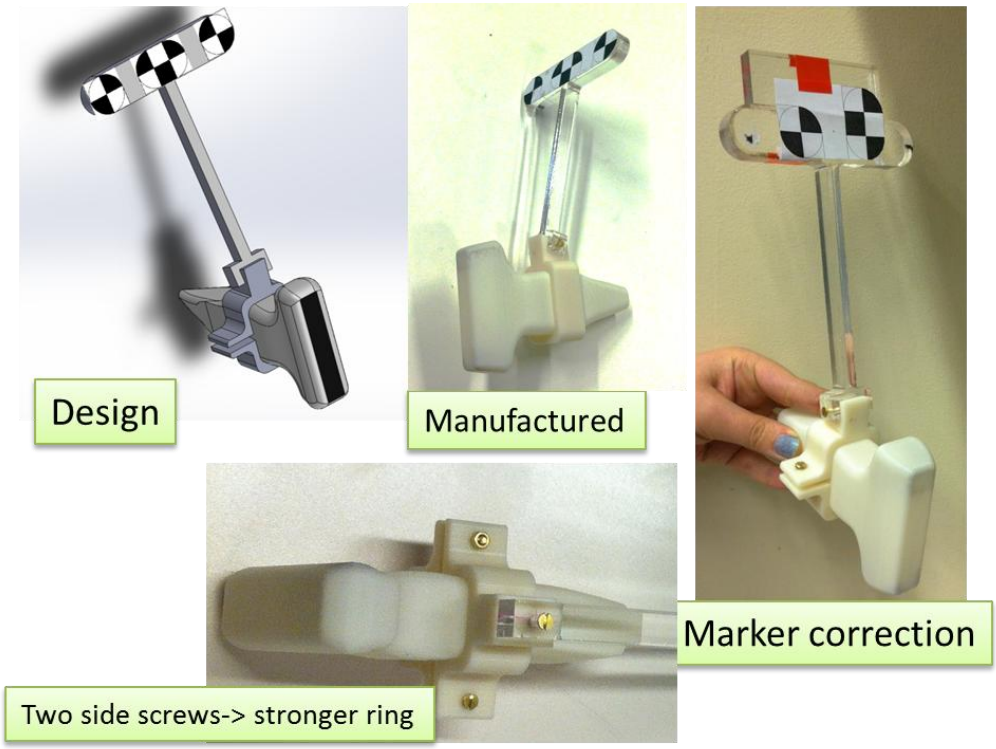


**Figure 5. Design and manufacturing of probe holders**

### 3.1.3 Endeffector

Robodoc has its own endeffector. In order to attach the tracker's camera and robot operated probe, we designed and manufactured a separate endeffector which could be mounted on the robodoc. Figure 6 shows the designed end effector attached to robodoc. Please refer to section 3.2.2 for explanation of the reason of such a design.

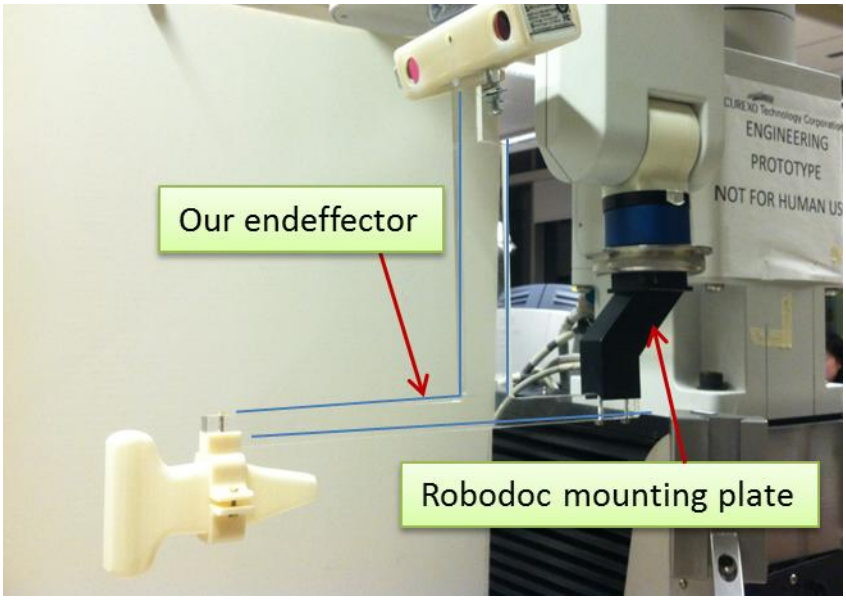


**Figure 6. Endeffector attached to robodoc mounting plate**

### 3.1.4 Pointer

For calibration purposes, a pointer compatible with MicronTracker was required. We built a sharp pointer using laser cutter (acrylic material) and a sharp pin. In order to calibrate the pointer, its tip should be placed in the center of a known marker (for example, manufacture calibrated TTblock marker as shown in Figure 7), and then the MicronTracker demo can automatically register the pointer marker to its tip.

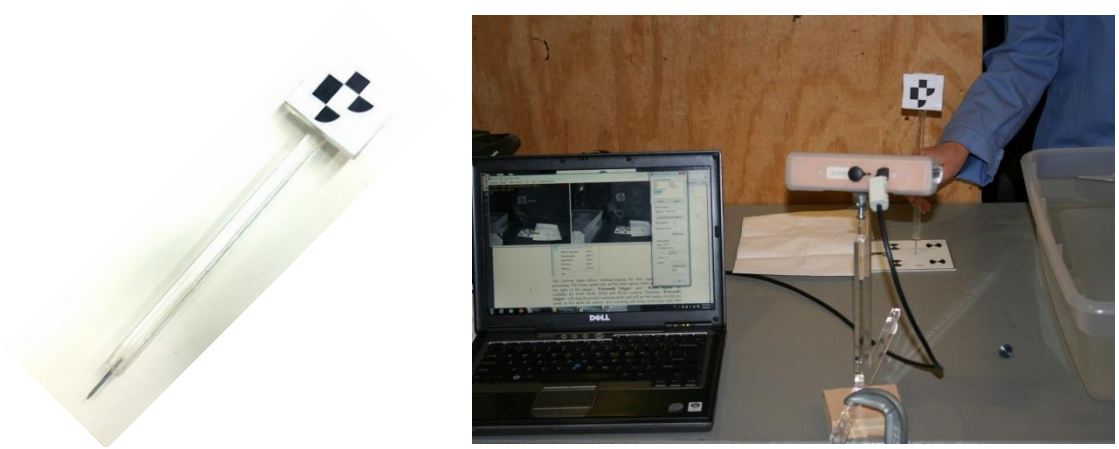

**Figure 7. Pointer and its calibration procedure using MicronTracker**

## *3.2 Tracking system*

One of the most important parts of this project is to have the two probes properly aligned. To make sure the system has an adequate accuracy, three loops of tracking are proposed: Tracker alignment, B-mode image alignment, and energy profile tracking (EPT). Tracker alignment is done using an external tracking system such as an optical or an electromagnetic tracker. B-mode

image alignment is accomplished by aligning the B-mode images of the two probes. Figure 8 shows two probes with misaligned B-mode images. The third loop of tracking is based on the energy distribution of the ultrasound waves. The ultrasound wave energy is not equally distributed in the space. This property can be used to align the probes more accurately by aligning the peaks as shown in Figure 9.

**Figure 8. B-mode image mis-alignment**

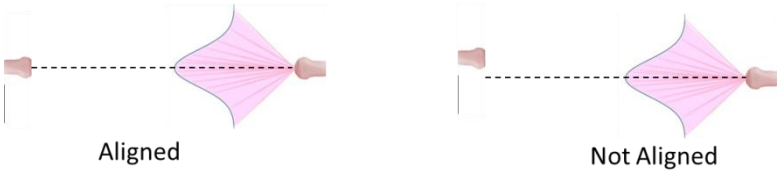


**Figure 9. Energy profile tracking**

In this project, we have implemented a combination of the first two tracking loops and have studied the feasibility of the third one through an experiment.

The first thing to consider for the external tracker is finding an appropriate place for it in the system's workspace. We chose to put the tracker on robot arm which has the following advantages:

- No limitation in workspace due to tracker's limited FOV
- Can have tomographic images from tracker to compensate for truncated tomography caused by small FOV of ultrasound image
- System will be more easily portable

Considering the above tracker placement, one may consider electromagnetic tracker as a better option over optical trackers since it does not require line of sight. However, electromagnetic tracker cannot provide tomographic images of the tissue. Hence, we selected MicronTracker which provides real-time images of the scene (visible light functionality), is small size and ultra-light (camera + case ~ 500 grams), has passive, easily printable markers and low cost stereo cameras.

MicronTracker has an accuracy of 0.23 mm RMS and its field of measurement is 120x120x90 mm for Hx40 model used in this project. The field of measurement for four different models of MicronTracker is shown in Figure 10.

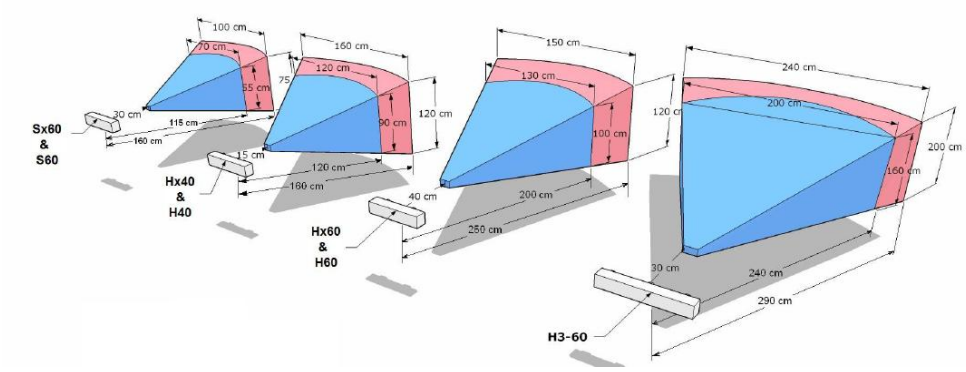


**Figure 10. MicronTracker FOMs for four different models from [6]**

### 3.2.1 MicronTracker markers

MicronTracker uses balck-white printed markers. Each marker consists of at least two facets. A facet is a vector connecting centers of two xpoints. An xpoint consists of x-shape white and black regions as shown in

Figure 11. Marker design for MicronTracker is the art of combining xpoints in different ways to produce different markers. The standard diameter of an xpoint is 2.4 cm which is a requirement to have the above mentioned FOM volumes.

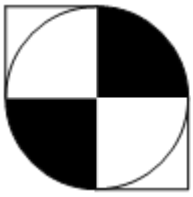

**Figure 11. An xpoint**

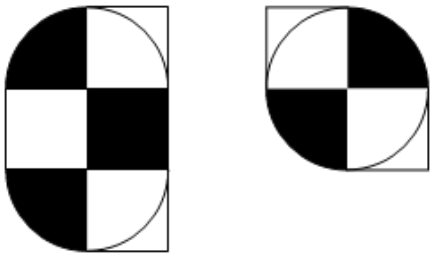

**Figure 12. Freehand probe marker**

### 3.2.2 MicronTracker rigid body designs

MicronTracker has the line of sight problem as mentioned above. This problem is illustrated in Figure 13. In summary, if the cameras are put aligned with the robotic probe, and the markers are directly attached to the freehand probe, the phantom will be obstructing the field of view. Hence an appropriate configuration should be found that can both address the line of sight issue and make sure that the marker is always in the field of view of the cameras.

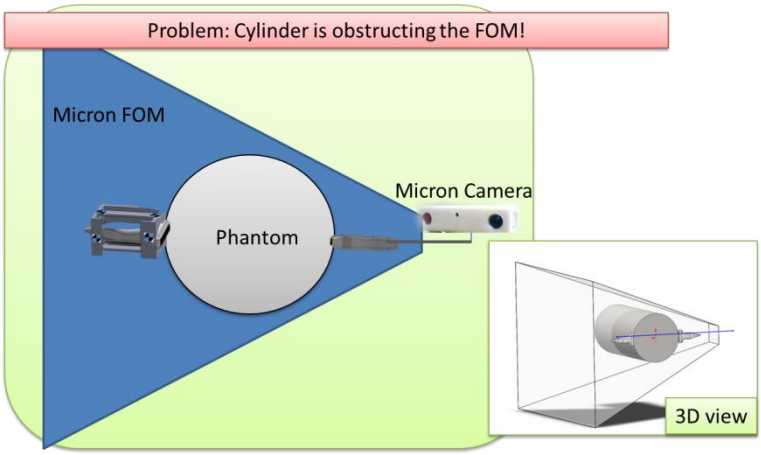


**Figure 13. Line of sight problem**

We created a simulated setup in Solidworks as shown in Figure 14. The success criteria are: 1. the freehand marker is in the cameras' FOM volume, and 2. the line connecting the center of cameras to the freehand marker center does not intersect with a cylinder of diameter 30 cm. It is found that if the camera is put at a height of 25 cm from robotic probe and marker is attached at a height of 12.5 cm from the freehand probe, then the success criteria are satisfied. In addition we considered tilting the camera 17 degrees to cover a larger part of the cylindrical phantom to get a better tomographic image.

Please note that we did the simulation for Sx60 model while due to unresolved dependency Hx40 was used in the project. However, migrating from Sx60 to Hx40 would keep the simulation result valid because the Hx40's FOM volume is larger than that of Sx60.

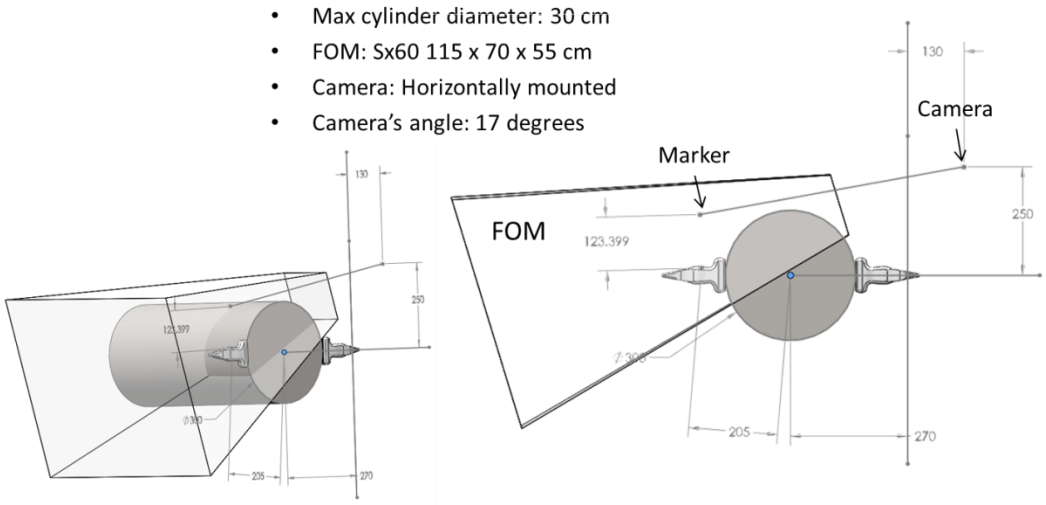


**Figure 14. Rigid body placements simulated in Solidworks**

### 3.2.3 MicronTracker calibration

MicronTracker comes with automatic calibration software called RFine. This software helps recalibrate the cameras without the need to send them to the company. The calibration should be

done every few months or when the cameras are put under hazardous conditions. We used RFine to calibrate the MicronTracker and the results showed an improvement of %34 as shown in Figure 15.

In addition, MicronTracker ships with a coolcard that is used for automatic adjustment of light coolness. The coolcard should be flashed over the cameras at the beginning of each measurement session.

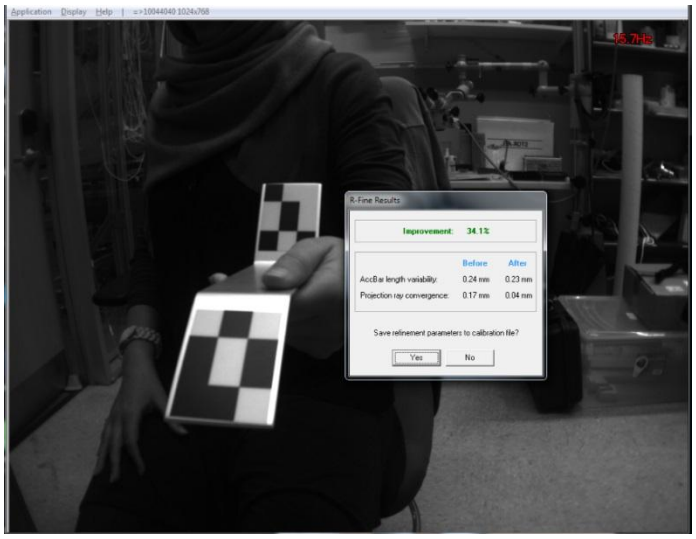


**Figure 15. RFine MicronTracker calibration**

### 3.2.4 MicronTracker Connection to PC

MicronTracker communicates with PC through IEEE 1394 port. We ordered StarTech 4-Port PCI 1394a FireWire Adapter Card with Digital Video Editing Kit and installed it on the PC. The PCI card is shown in Figure 16.

**Figure 16. 4-port PCI 1394a Firewire**

### 3.2.5 MicronTracker software

MicronTracker has a user-friendly demo software in which markers can be easily registered, pointers can be calibrated, and tracker data can be recorded as positions, angles, or transformations.

MicronTracker provides MTC libraries for code developers. Some simple API's are available in C, C++, C#, and other languages. In this project we used simpledemoc sample code.

## *3.3 Robot*

### 3.3.1 Robodoc

The type of robot required for complete motion following of a free hand probe is a 6 degree of freedom robotic arm but due to infrastructure limitations, we finalized on Robodoc, a 5 degree of freedom with the main function of being used as a Miller in total knee and hip replacement surgeries. As the robot we finalized is a 5 degree of freedom robot, we have to forgo one degree of freedom which it cannot follow. The axis that we forgo of is the roll axis (due to Robodoc design limitations).

The degrees of freedom of the different links of the robot are:

Link 1 → Rotation along z – axis
Link 2 → Rotation along z – axis
Link 3 → Translation along z – axis
Link 4 → Rotation along y – axis
Link 5 → Rotation along z – axis

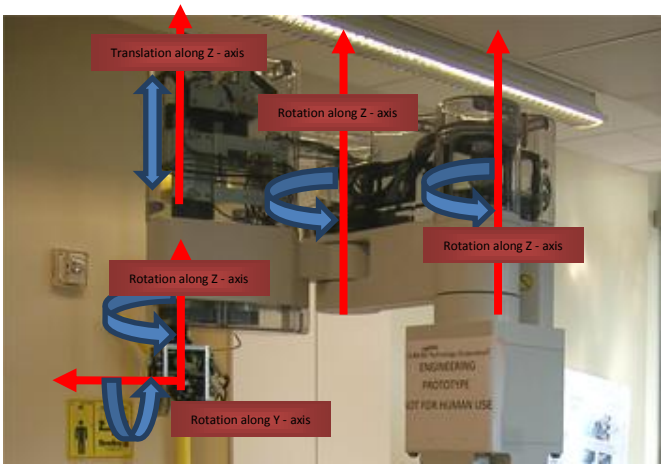


**Figure 17. Different DOF of Robodoc**

The coordinate axis of the robot base is depicted in the image shown below.

For the robot, the coordinate axis are defined as follows:

| | |
|---|---|
| **X – Axis →** | **Red** |
| **Y – Axis →** | **Yellow** |
| **Z – Axis →** | **Blue** |

**Figure 18. Robodoc Coordinate Axis**

### 3.3.2 Simulator

In order to start working with the project, we were provided by a Robodoc simulator which does exactly what the real robot would do but in virtual world. We used the simulator to do all our trials and then we moved onto the real robot once we had our system working in the simulator.

The Simulator was provided to us by Dr. Peter Kazanzides.

From the simulator we got to know visually where our homing position is and it looks as follows:

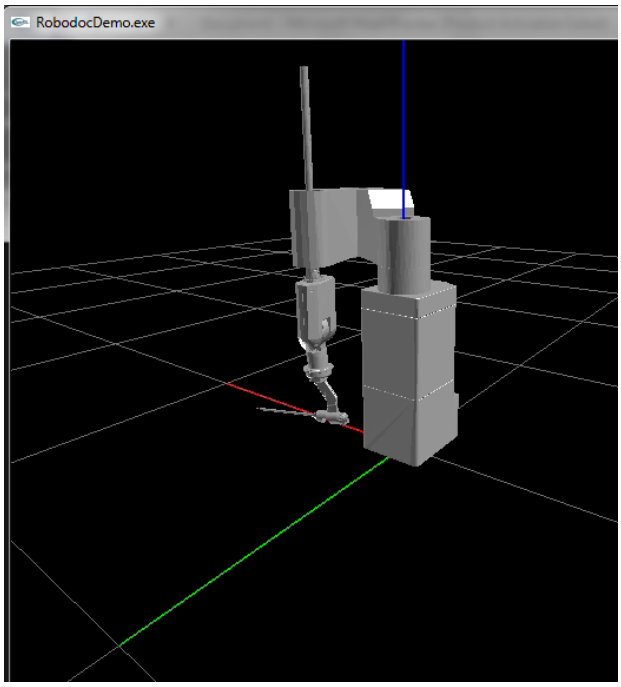


**Figure 19. Robodoc in Homing Position in Simulator**

The simulator is based on CISST and Open GL libraries. In order to run the simulator as well as the real robot, we have three different components running in tandem. They are:

- Cisst Gloabal Component Manager
- Robot Server
- Rododoc Demo

The Cisst Global Component Manager communicates with the Robot Server and the Robodoc Demo; and Robodoc Demo Communicates with the Robot Server.

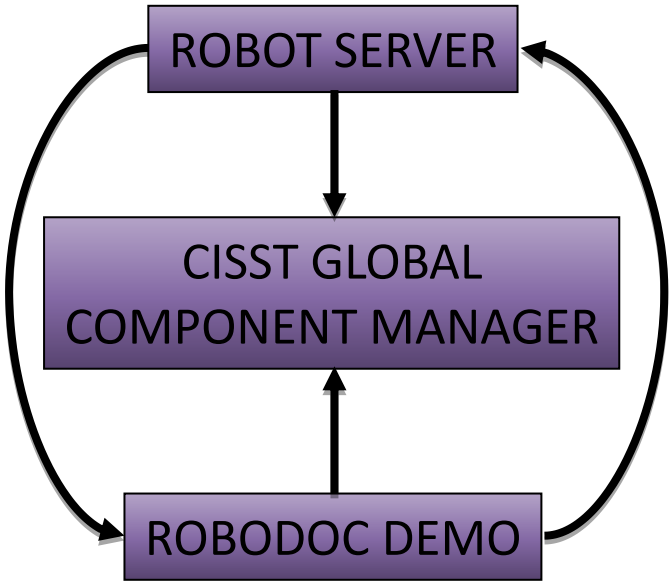


**Figure 20. Schematics of Simulator Components Communitcation**

The Robodoc Demo involves our algorithm implementation and in order to communicate with the robot, we need the robot server. We call predefined functions written in the robot server, in Robodoc demo which in turn cause effects on or from the robot.

After implementing our algorithm on the simulator and confirming that it worked correctly, we moved onto the real robot. The only difference between the real robot and simulator is that now we had to communicate with the robot server that communicates with the real robot and not the simulator.

## *3.4 Ultrasound imaging*

In ultrasound imaging, RF signals are sent through the medium and the reflected RF signals, which correspond to the convolution integral between the spatial density of tissue and the point spread function (psf), are processed to form the image [7]. Figure 21 shows four different data acquisition modes in ultrasound imaging:

1. Acquiring analog signal: The advantage is that this mode is available in almost all ultrasound machines. The disadvantage is that the frame rate is less than digital modes (less than 30 f/s) and also we need to convert it again to digital data to store on the external computer.
2. Three Digital modes: These digital data can be acquired at a faster speed (up to 100 f/s) and can be directly stored on the computer. These modes, however, need to be processed on the external computer to form a geometrical image.

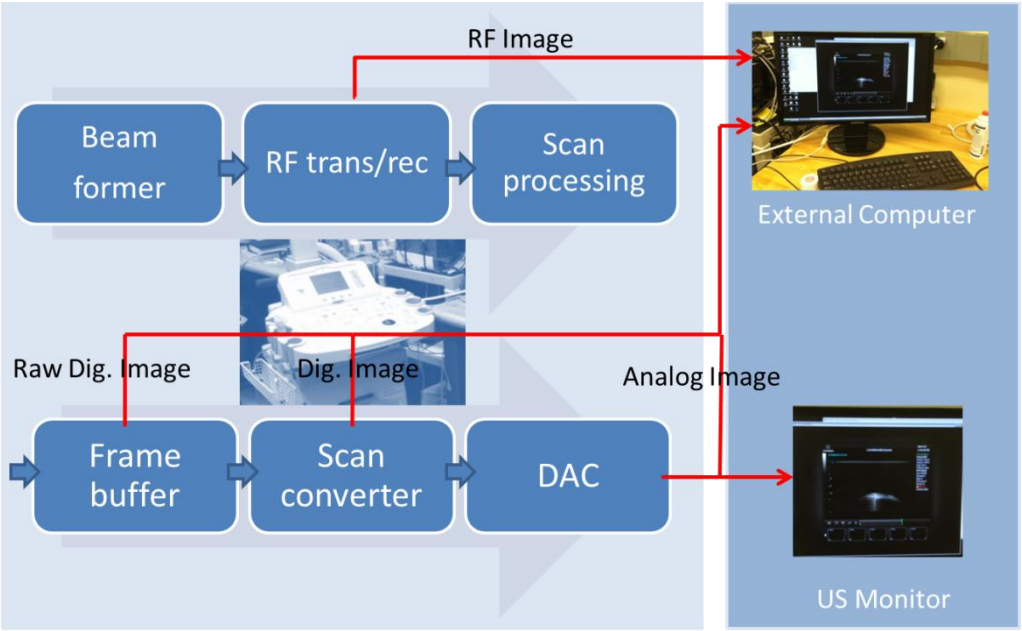


**Figure 21. Ultrasound machine image acquisition adapted from [7]**

In this project, we mostly used the digital B-mode image for ultrasound calibration. The image is accessible through research license and we stored 8-bit (.b8 type) images that can be imported into Matlab for further processing.

There are several important settings that need to be set for ultrasound imaging:

**Depth:** it determines the maximum penetration the ultrasound waves can travel to make the image. The imaging depth used in our application is 9 cm.

**Frequency:** frequency of the ultrasound waves which determines the image resolution. The more frequency, the better resolution image is acquired. In this project we used 6.6 MHz.

**Dynamic range:** it determines the intensity range of pixels. By varying the dynamic range, operator can get a better image at each time.

There are several other settings that can be changed during image acquisition; For example, it is possible to turn off some of the apertures, or change focus of the waves, magnify some part of image, etc.

## *3.5 Ultrasound calibrations*

In order to incorporate the B-mode image alignment, the transformation from the freehand probe marker coordinate system to its ultrasound image coordinate system is found through ultrasound calibration. On the other hand, the transformation from the tracker's camera coordinate system to the robot operated probe ultrasound image is found through another ultrasound calibration. Note that, since we used mock ultrasound probe on the robot side, a mock ultrasound calibration is carried out.

### 3.5.1 Method

We chose single point target pointer calibration method for the first ultrasound calibration. Details of a pointer calibration can be found in [8]. For a more developed method considering temporal calibration and an implementation on IGSTK please refer to [9] and [10] respectively. We used the simple pointer calibration method, i.e., a calibrated pointer tip is entered into the image plane from sides (Half of the samples were collected from right side and half from left side). Hence, the pointer tip will be the feature that is extracted from the ultrasound image.

Using MicronTracker, we are collecting the position and angle of the freehand probe marker, and the position of pointer tip in the tracker's coordinate system. Then through analysis, we find the position of pointer tip in the marker's coordinate system, and apply a point-to-point registration to get the unknown transformation. Please note that in this method, the probe needs to be kept fixed throughout the whole data collection which is done using a passive arm.

The advantages of the pointer calibration method are:

- It does not require phantom
- We do not need to worry about tracker's FOV and line of sight

The second advantage is especially valuable in our application due to small FOV of the MicronTracker. However, this method has rather less accuracy due to possible movement of hand during data collection, infeasibility of manual collection of a large set of data, and poor accuracy along the image thickness axis. In order to improve the poor accuracy due to hand movement, we used a passive arm to hold the pointer at each point and we collected 60 set of points. The reason for having a poor accuracy along image thickness axis (z-axis of ultrasound image coordinate system) is that, when the pointer enters the image from side, we are not sure where along the thickness the pointer is. In order to overcome this issue, it is possible to benefit from active echo element at the pointer tip which starts blinking whenever the pointer is in the center line of the image thickness. This can be a future work in the project.

### 3.5.2 Experiment setup

The experiment setup is shown in Figure 22.

**Figure 22. Ultrasound calibration experiment setup**

The following procedure is done to prepare the experiment setup:

1. Fix the probe inside a water tank such that all the US arrays are in the water
2. The probe has a marker attached to it and this marker is fixed at a height with respect to the probe so that it is outside the water tank.
3. The probe is fixed with respect to camera.
4. A camera (tracker) is fixed on top-side of water tank such that it can see the marker attached to the probe.
5. A sharp pointer is used and the pointer tip is registered to the tracker offline.
6. The tracker is connected to the laptop and a software tool can record position of pointer tip and position and angle of probe marker by pushing a button.
7. The ultrasound machine is set in research mode and the depth is set to 9 cm; the focus is at the pointer tip point. Dynamic range, gain, active apertures, etc. are set such that the pointer tip is its best visibility in the image.

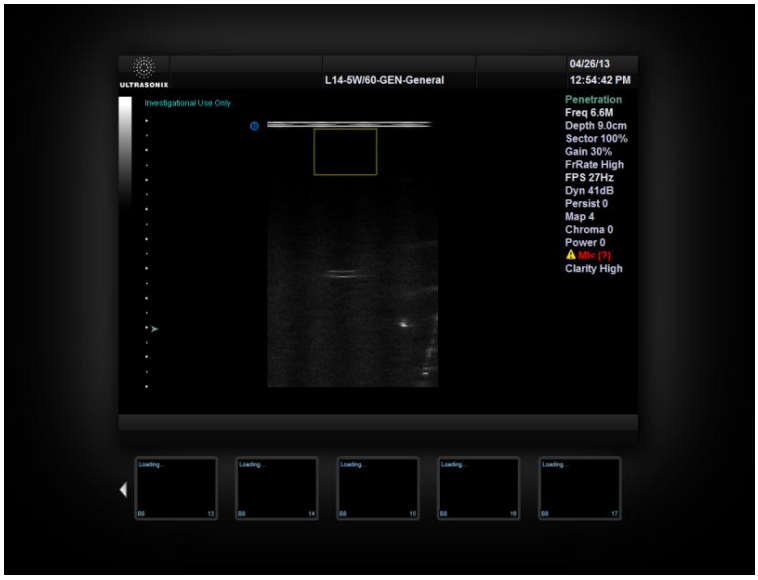


**Figure 23. Screenshot of main settings for ultrasound calibration image acquisition**

8. Ultrasound image is captured using Print1 button and storing the last 10 frames as .b8 file.
9. We move the pointer tip into the US image and once a light point is seen, the tracker "Record Stream" button is pushed. The pointer is kept as still as possible using a passive arm during the data collection. The passive arm also helps making sure the data from ultrasound machine is synchronized with the data from tracking system. After more than 10 frames are captured by the tracker, the ultrasound recording button is pushed. The US machine records the past 54 frames but frames 45 to 54 are only stored as the protocol of data recording. We take the average over this set of data and label it as one point of data collection to have a better accuracy. In addition, since the US frames are rather large, storing only the last 10 frames helps avoid storing a large data and can speed up the segmentation process.
10. We repeated that for 60 times and hence we have 60 set of points, each set contains:
    a. 3D position of pointer tip in camera space
    b. 2D position of pointer tip in US image
    c. Transformation from camera to probe's marker
11. The 3D position of pointer tip is ready to use from tracker's recorded data.
12. The transformation from camera to probe's marker is not readily available in tracker's recorded data. In fact, the tracker only stores the positions and angles of marker coordinate system in camera space (It is possible to collect transformation matrix directly but it was not done in our data collection). Hence the transformation matrix should be calculated:

$$transformation = Rz.Ry.Rx$$

When we have the transformation from camera to marker, we find the position of pointer tip in marker's coordinate system. Note that although the probe's marker is fixed, it could have some little movements (possibly) and we found the location of pointer tip in the average probe marker coordinate system each time.

13. The 2D points in the image is extracted using the following method:
    a. Convert the b8 file into matrix using uread function downloaded from [11].
    b. The 10 frames are averaged
    c. Then the arrays that contain the highest intensity are found and average of their 2D position in image is considered as the pointer tip. Figure 26 shows a sample of pointer tip found with this method.
    d. The, the x-axis data is shifted by half of the number of pixels in x-axis to place the origin of the x-axis at the center-top of the image.
    e. The pixel size is calculated by dividing the number of pixels along y-axis by 90 mm.
    f. Apply speed of sound compensation:

Speed of sound is assumed 1540 m/s (speed of sound in human tissue) in ultrasound machine and the measure distance is calculated as below:

$$d_{measured} = propagation\ time \times \frac{1540}{2}$$

However, during US calibration coupling medium is water; so the measured distance should be adjusted to find the real distance. Figure 24 shows what happens if the speed of sound compensation is not done and Figure 25 shows the formula to find the real distance.

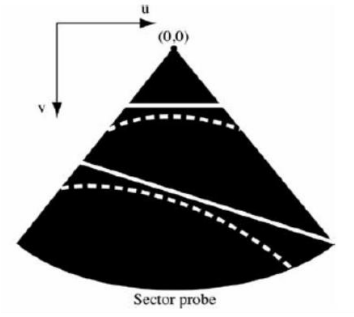


Image from: L. Mercier, et. al, A review of calibration techniques for freehand 3d ultrasound

**Figure 24. Speed of sound issue**

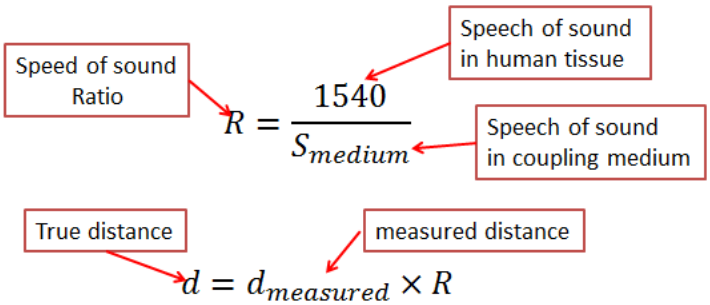


**Figure 25. Speed of sound compensation**

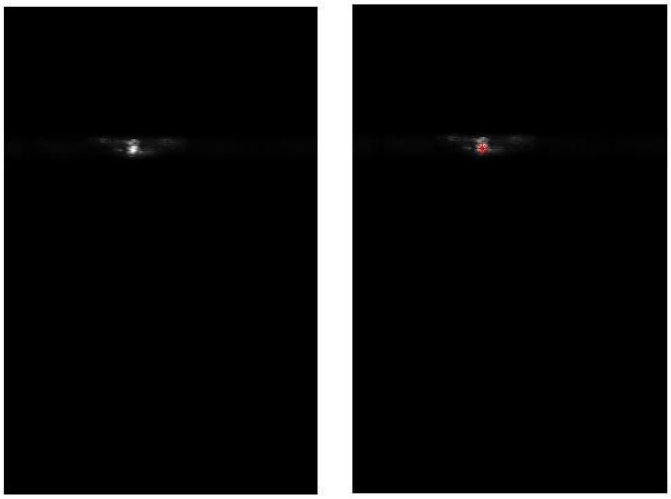

**Figure 26. A sample ultrasound calibration image with the pointer tip visible and red point in the right image is the point detected through auto-segmentation**

### 3.5.3 Results and evaluation

We had to discard four sets of data due to incomplete reading from ultrasound machine or tracker. Here is the result from 54 data sets:

| | |
|---|---|
| Standard deviation of probe position (mm) | [0.2384 0.2539 1.0596] |
| Transformation from marker coordinate system to ultrasound image coordinate system | $\begin{bmatrix} 0.2844 & -0.2335 & -0.9298 & 17.2292 \\ 0.8520 & -0.3832 & 0.3568 & -191.5770 \\ -0.4396 & -0.8937 & 0.0899 & -36.6060 \\ 0 & 0 & 0 & 1 \end{bmatrix}$ |

For evaluating the accuracy and precision of the ultrasound calibration, we used a cross wire phantom inside a water tank with rubber sides. The probe was used to image the cross point from different angles through the rubber.

We want to find the position of the fiducial in the camera coordinate system several times as shown in Figure 27 using X, transformation matrix found through US calibration, and find the standard deviation. This will give us the precision. The fiducial position should ideally be always the same in the camera space as they are fixed during the experiment. In order to measure the accuracy, the position of the cross point is evaluated using the calibrated pointer.

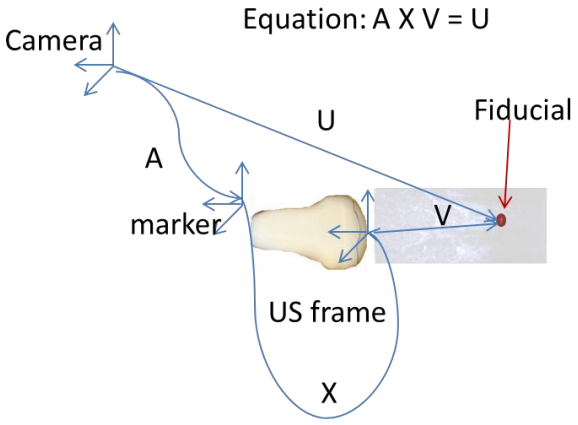


**Figure 27. Ultrasound calibration evaluation**

We collected 7 sets of data similar to the above procedure and we did similar data processing to extract the 2D positions of the point in the US image and camera-marker transformations.
Now we have the probe's marker transformations, and the 2D positions of fiducial in US image and X (from previous experiment). We append [0 1] to the end of 2D positions and call it V, and calculate position of fidcial in camera space.

| | |
|---|---|
| Standard deviation of the points cloud (mm) **(precision)** | [4.3467 1.2044 1.3065] |
| Mean of the points cloud (mm) | [37.3689 86.5109 479.2239] |
| Pointer position (mm) | [32.9422 90.9091 471.5404] |
| Mean of error (cloud points vs. pointer) (mm) **(accuracy)** | [-4.4267 4.3982 -7.6835] |

An observation is that the reason for having a poor precision along x-axis in version 2 calibration is the image thickness. Because we could see that the pointer_tip_x in camera coordinates is varying from -30 to 30 mm.

### 3.5.4 Mock Ultrasound calibration

To mimic the ultrasound calibration for the mock probe, we used a cardboard with two points one in the y-axis and one on the x-axis. We used the calibrated pointer to find the position of these two points and the probe tip center point in the camera coordinate system. If the point's 3D position on the x-axis is called *X*, the point's 3D position on the y-axis is called *Y*, and the 3D position of the probe tip center is called *origin*, then the transformation from camera to probe tip, *T* is as follows:

$$T = [T'_1 T'_2 T'_3 T_4']$$

Where $T'_1$ is transpose of $T_1$:

$$T_1 = [\frac{origin - X}{|origin - X|}\ 0]$$

$$T_2 = [\frac{origin - Y}{|origin - Y|}\ 0]$$

$$T_3 = X \otimes Y$$

$$T_4 = [origin\ 0]$$

The resulting transformation is when x-axis is up, y-axis is outside the probe, and the coordinate system is left-handed:

$$\begin{pmatrix} -0.0271 & -0.0480 & 0.9985 & -3.2275 \\ -0.9512 & -0.3014 & -0.0406 & 217.5360 \\ -0.3073 & 0.9523 & 0.0375 & 313.1950 \\ 0 & 0 & 0 & 1.0000 \end{pmatrix}$$

## *3.6 Hand-eye calibration*

Hand Eye Calibration is the calibration to get the transformation between Robodoc's tool tip and the MicronTracker. The reason we are looking at this transformation is because Robodoc is used to perform milling in total knee and hip replacement surgeries and Robodoc is specifically calibrated to use the tool tip as its end effector, in other words, the tool tip is the point that is in placed at (x,y,z) coordinates if given the command to move the robot to (x,y,z) coordinates with respect to robot base. The point to note here is that MicronTracker is not fixed in the world coordinates, it keeps on moving with the robot end effector as it is attached to it but we know by design that the tool tip of the robodoc will always be at a constant pose with respect to the MicronTracker and vice-versa.

### 3.6.1 Method

This problem of finding the transformation is done using AX = XB method.

The easiest way to explain this is by taking an example transformation diagram of two different poses, pose 1 and pose 2. We know the following:

- The Robot base is fixed.
- The marker is fixed in world coordinates at such a position that it can be viewed by the MicronTracker in various different poses.
- The position and orientation of the marker can be read in MicronTracker coordinates in pose 1 and pose 2 given as $\mathbf{B}_1$ and $\mathbf{B}_2$.

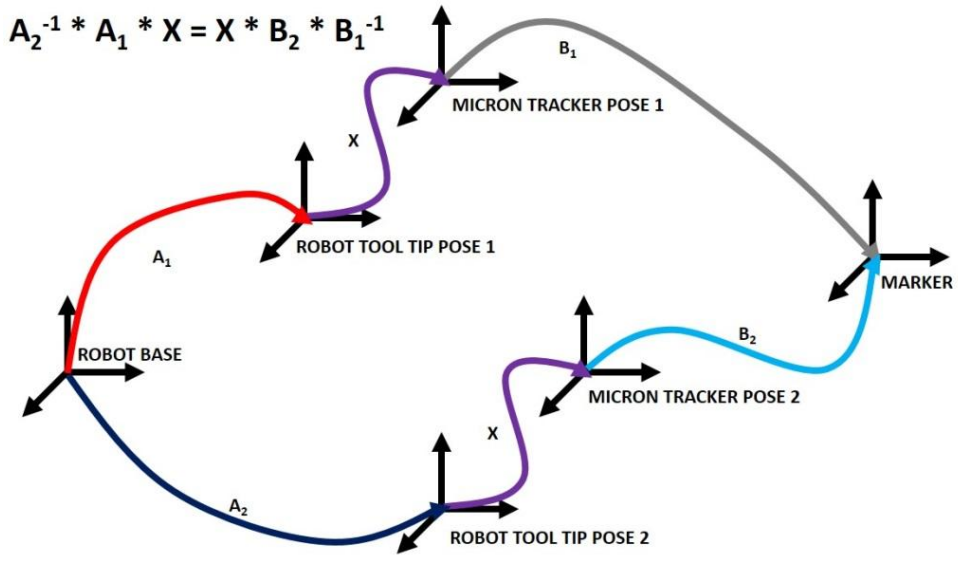


**Figure 28. Hand Eye Calibration Transformation Diagram**

- The position of the robot tool tip can be read through the encoders and stored as $\mathbf{A_1}$ and $\mathbf{A_2}$ for two different poses.
- The transformation between the robot tool tip and MicronTracker is always fixed for all poses through design and is labeled as **X**.

Now, through this system if we take readings for multiple poses and record them, we get the typical **AX = XB problem** which we learnt to solve in CIS1:

$$\mathbf{A_k = A_j^{-1} * A_i}$$

$$\mathbf{B_k = B_j * B_i^{-1}}$$

where **i,j,k € R.**

We find **X** using a Matlab code for solving the **AX = XB problem.**

### 3.6.2 Experiment setup

The experimental setup was as follows:

- A marker was placed at a fixed point in the world.
- The robot was working in cooperative mode. It was moved to a pose where the MicronTracker can view the marker clearly.
- The readings were taken from the MicronTracker and the robot's encoders to get the A's and B's as explained above.

### 3.6.3 Results and evaluation

We had 10 poses with different readings of A and B, from those we get the resulting transformation as:

$$\begin{pmatrix} -0.1019 & 0.2707 & -0.9838 & -318.2332 \\ 1.0241 & 0.0198 & -0.1156 & -17.1154 \\ 0.0254 & -0.9902 & -0.2682 & 280.6833 \\ 0 & 0 & 0 & 1.0000 \end{pmatrix}$$

For evaluating the accuracy of the transformation, we use the same setup and using the transformation move the robot's end effector to that point where the marker is placed. The MicronTracker looks at the marker, we compute the motion of the robot with MicronTracker's reading as goal position. Then we check using pointer the difference between the current position of the robot's end effector and the position of the marker, the difference between them gives us

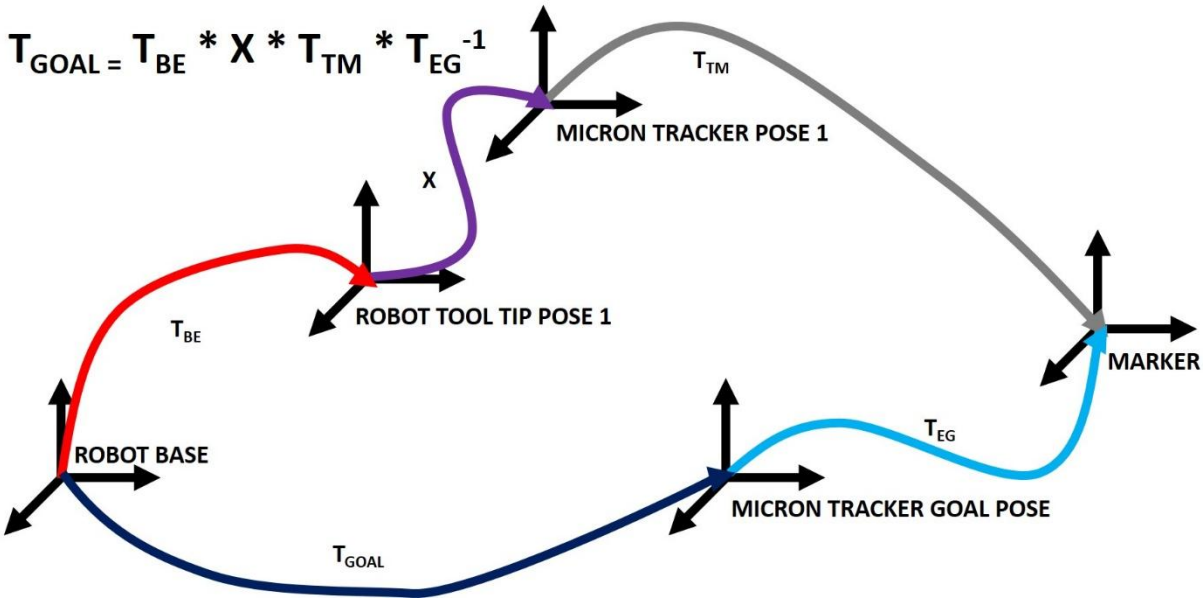


**Figure 29. Hand Eye Calibration Evaluation**

the error.

The accuracy is as follows

[ 2.8921 4.7664 -3.7125 ]

Repeatability has the error as follows

[0.0460 0.3360 0.4950 ]

## *3.7 Software development*

The code is written entirely in C++ and uses CISST libraries. The code utilizes the knowledge of the entire system to produce the goal positions corresponding to the knowledge of the world provided by the Micron Tracking System. The best way to explain the entire system is through a transformation diagram as shown below:

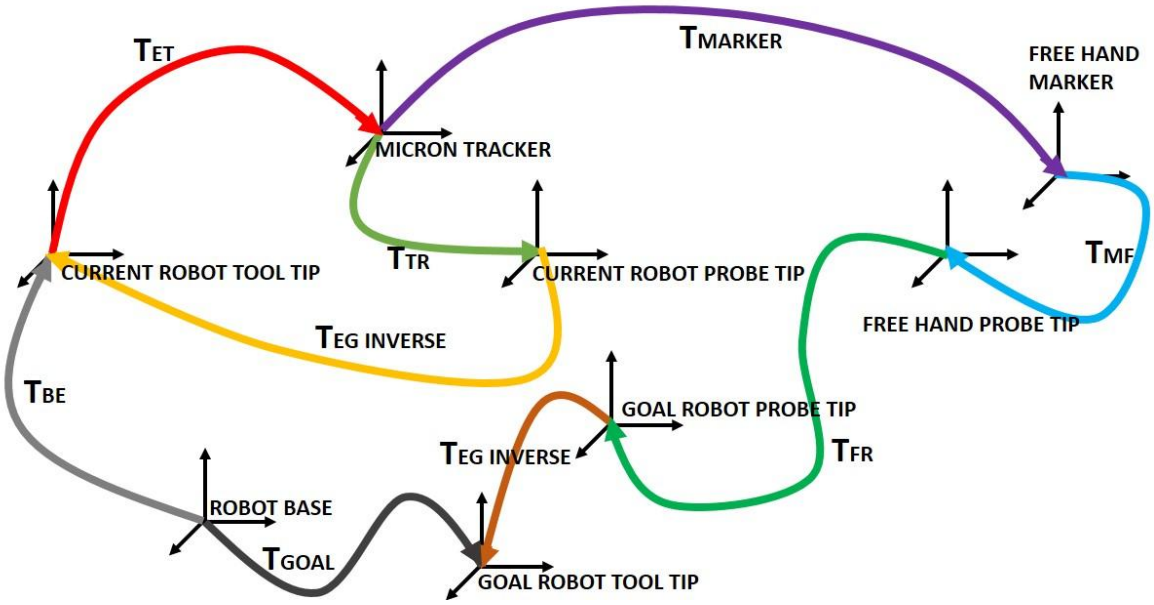


**Figure 30. Transformation Diagram of the System**

Where,

- $T_{BE}$ → Current Tool Tip Transformation with respect to Robot Base
- $T_{ET}$ → Transformation Between Tool Tip and the MicronTracker
- $T_{MARKER}$ → Transformation Between MicronTracker and Free Hand Probe Marker
- $T_{MF}$ → Transformation Between Free Hand Probe Marker and Free Hand Probe Tip
- $T_{FR}$ → Transformation Between Free Hand Probe Tip and Goal Robot Probe Tip
- $T_{TR}$ → Transformation Between MicronTracker and Robot Probe Tip
- $T_{EG\ INVERSE}$ → Transformation Between Robot Probe Tip and Robot Tool Tip

We get these Transformations as follows:

- $T_{BE}$ → Through robot encoders
- $T_{ET}$ → Through hand eye calibration
- $T_{MARKER}$ → Through MicronTracker
- $T_{MF}$ → Through ultrasound calibration
- $T_{FR}$ → Through cylindrical phantom design
- $T_{TR}$ → Through mock ultrasound calibration
- $T_{EG\ INVERSE}$ → Through the equation mentioned below after getting the above transformations

$$T_{EG\ INVERSE} = T_{TR}^{-1} * T_{ET}^{-1}$$

Now to find the goal position of the robot we make use of all the transformations mentioned above and substitute them in the formula:

$$T_{GOAL} = T_{BE} * T_{ET} * T_{MARKER} * T_{MF} * T_{FR} * T_{EG\ INVERSE}$$

### 3.7.1 Structure of the Code

In the code we have implemented a switch case, i.e. we can choose from various options. The options are as follows with their functionalities:

- **QUIT**
  Used to quit the program
- **HOMING THE ROBOT**
  Used to move the robot to its homing position
- **MOVE ROBOT TO WORKSPACE VIEW**
  Used to move the robot such that the MicronTracker views our experimental setup
- **COMMENCE FREE HAND PROBE FOLLOWING**
  Used to start implementing the algorithm for probe following
- **STARTUP**
  Used to start up, i.e. power up the robot
- **SHUTDOWN**
  Used to shut down the power of the robot
- **STOPMOVE**
  Used in case we want to stop any motion of the robot being carried out
- **GET CURRENT POSITION**
  Used to get the current position of the robot in Cartesian space with respect to robot base
- **MOVE ROBOT TO ANOTHER POSE**
  Used to move the robot to a different configuration for trial cases
- **TEST ACCURACY OF HAND EYE CALIBRATION**
  Used when we wanted to perform the accuracy of hand eye calibration

Figure below shows how the interface looks with the simulator and different cases to choose from:

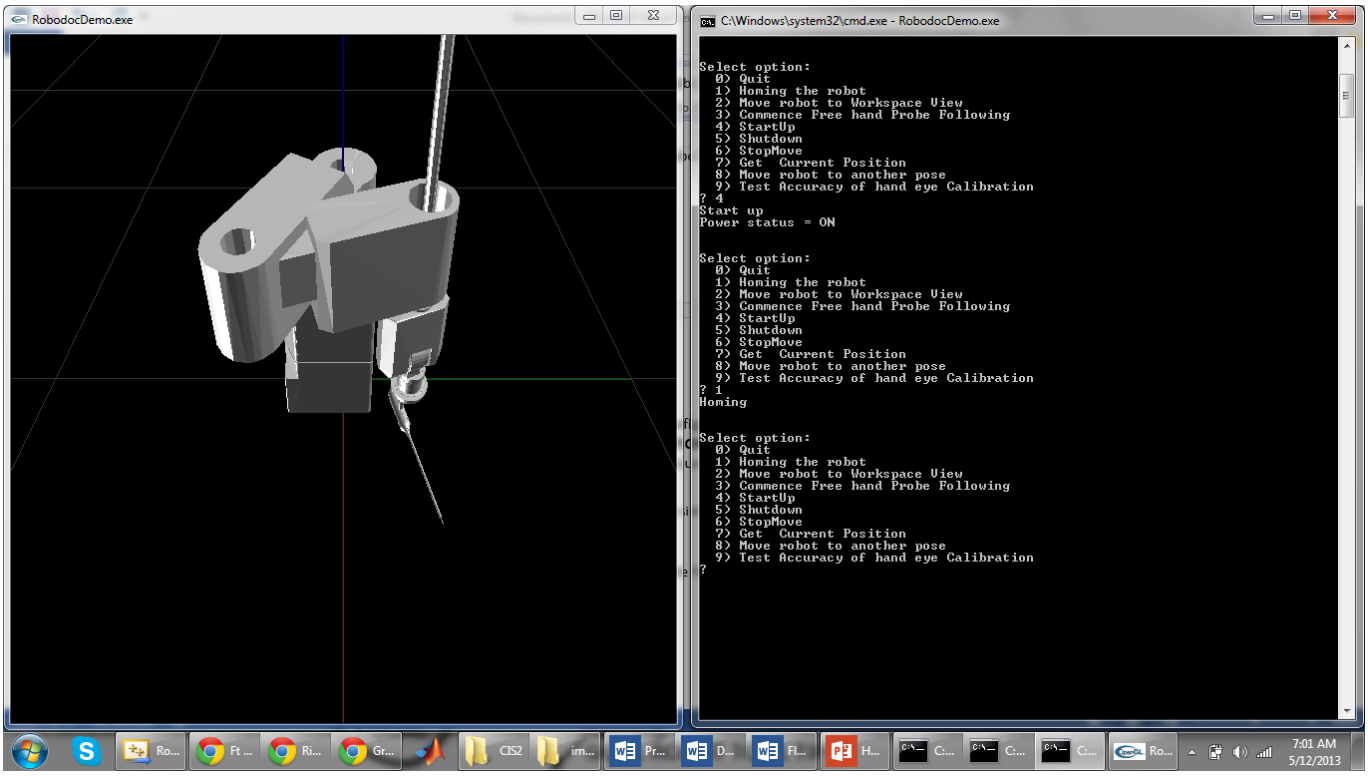


**Figure 31. Simulator Interface**

The algorithm for case 3, i.e. robot probe following the free hand probe implementation is best explained through the flow chart below:

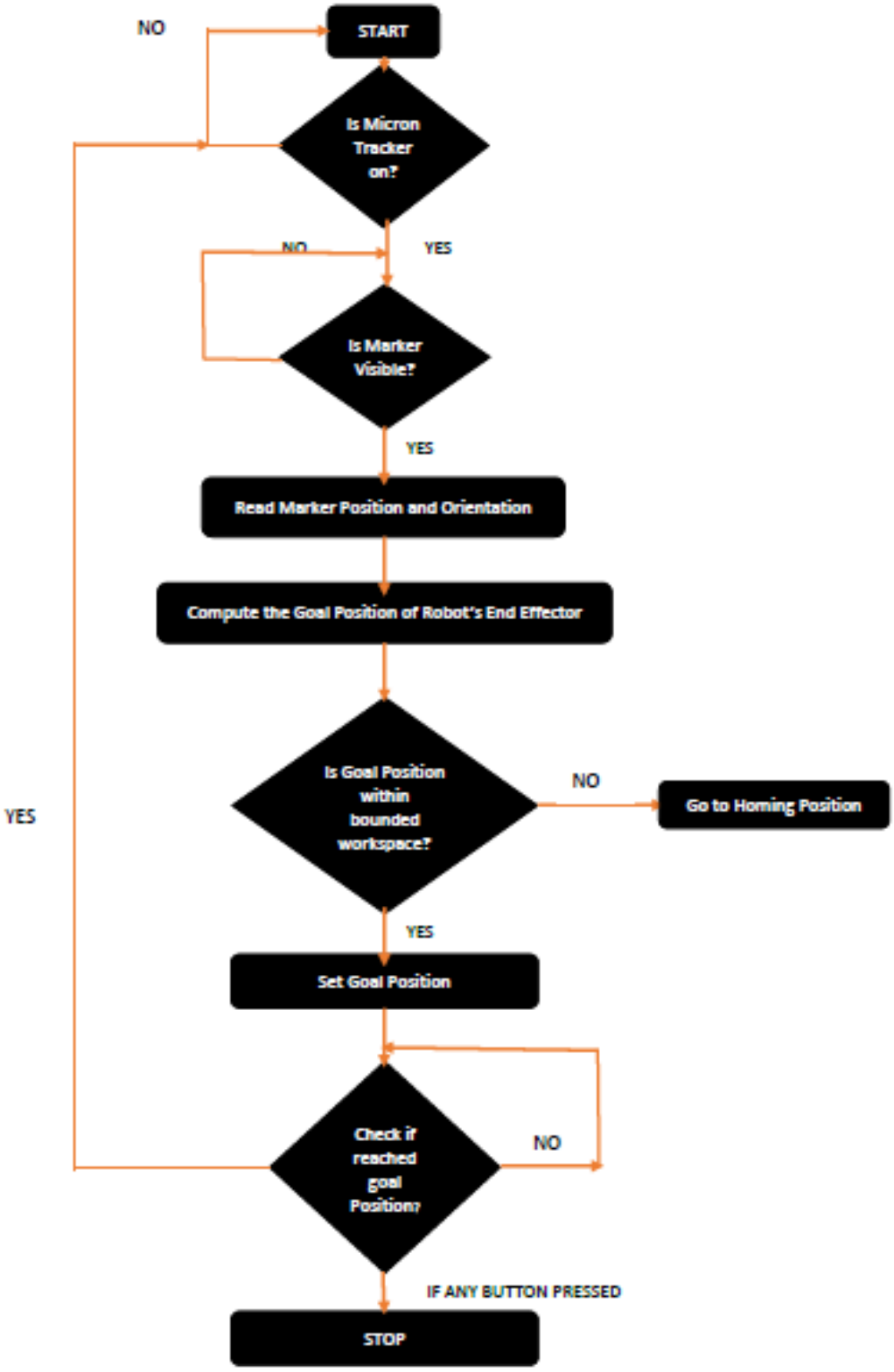


**Figure 32. Flow Chart for Trajectory Tracking Algorithm**

### 3.7.2 Safety Features

There are a few safety features in or added to the system in order to safeguard the people standing around as well as the patient:

- The workspace is predefined and if a goal position is encountered that is outside this workspace, we stop every motion and move back to the initial workspace view pose of the robot and break out of the trajectory tracking loop.
- There are inherent force sensors of the Robodoc which turn the robot off if a force threshold is crossed.
- If the marker is not visible to the MicronTracker, the robot stops moving and dose no motion until the marker is again visible.
- If we feel that there is something wrong, we can quit out of the loop by pressing any keyboard key which stops any robot motion that is going on and breaks out of the loop.

## *3.8 Experiment setup*

Experiment setup refers to placement of different components of our system. The different system components are:

1. Robodoc
2. 1 End effector with 1 MicronTracker and 1 mock probe attached
3. 1 Cylindrical phantom and tripod stand for base
4. 1 Real Ultrasound Probe

Now there are a lot of things that were kept in mind before finalizing the setup of the experiment, they were:

- Dexterous workspace of the robot, i.e. the place where the robot's end effector can move around with maximum accuracy.
- Limitations of the actual workspace due to size of the end effector. This limitation is mostly because Robodoc can move only 250 mm along the z-axis.
- Positioning the phantom at such a place that the MicronTracker can view the marker on the free hand probe clearly from the initial starting position.
- Keeping the phantom stable throughout the experiment by having a stable base on which it is placed for the experiment

Based on the above mentioned clauses, we place the cylindrical phantom as shown below in the figure such that the robodoc's end effector is always in the dexterous workspace.

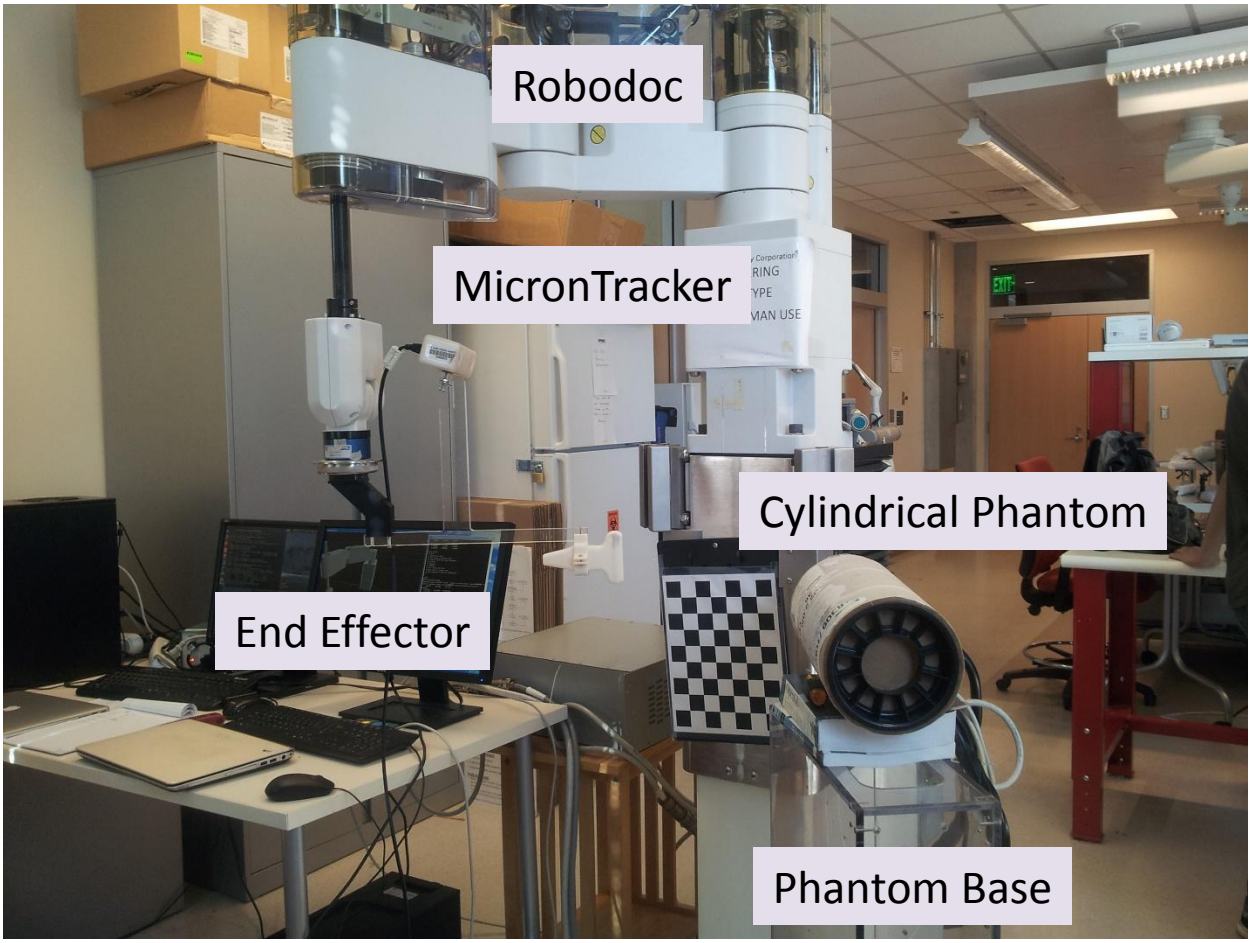


**Figure 33. Experiment System Setup**

In order to run the system, we do the following steps:

1. Run Cisst Global Component Manager
2. Run Robot Server that communicates with the robot.
3. Run the Robodoc demo exe file which shows up a window of the simulated robot and the different choices to choose from.

The steps followed to run the algorithm for robot probe following the free hand probe are:

1. Start the robot by pressing 4
2. Go to Homing position by pressing 1
3. Go to the position from where you can view the workspace by pressing 2
4. Start the loop for free hand probe trajectory tracking by pressing 3
5. Whenever you want to quit, press any button on the keyboard to come out to the main menu from where you can choose again what to do.

### *3.9 Results and evaluation*

The experiment was carried out and visually we could notice that the robot probe follows the trajectory of the free hand probe as mirror image with an accuracy of about 5 mm rms. There are various parameters that affect the overall accuracy of the system which have been discussed in detail above. To put them in tabular form, they are as follows:

- Accuracy of the Robot
- Accuracy of $\mathbf{T_{ET}}$, transformation between the Robodoc tool tip and the MicronTracker
- Accuracy of the MicronTracker, i.e. $\mathbf{T_{MARKER}}$, transformation between the MicronTracker and the marker on the free hand probe
- Accuracy of ultrasound calibration, i.e. $\mathbf{T_{MF}}$, transformation between the marker of free hand ultrasound probe and the ultrasound probe tip
- Accuracy of $\mathbf{T_{TR}}$, transformation between the MicronTracker and the robot mock ultrasound probe tip
- Accuracy of $\mathbf{T_{EG\ INVERSE}}$, transformation between the robot probe tip and the Robodoc tool tip

As we know the above values mentioned, we can find the overall expected accuracy of the system by substituting in the transformation diagram as follows:

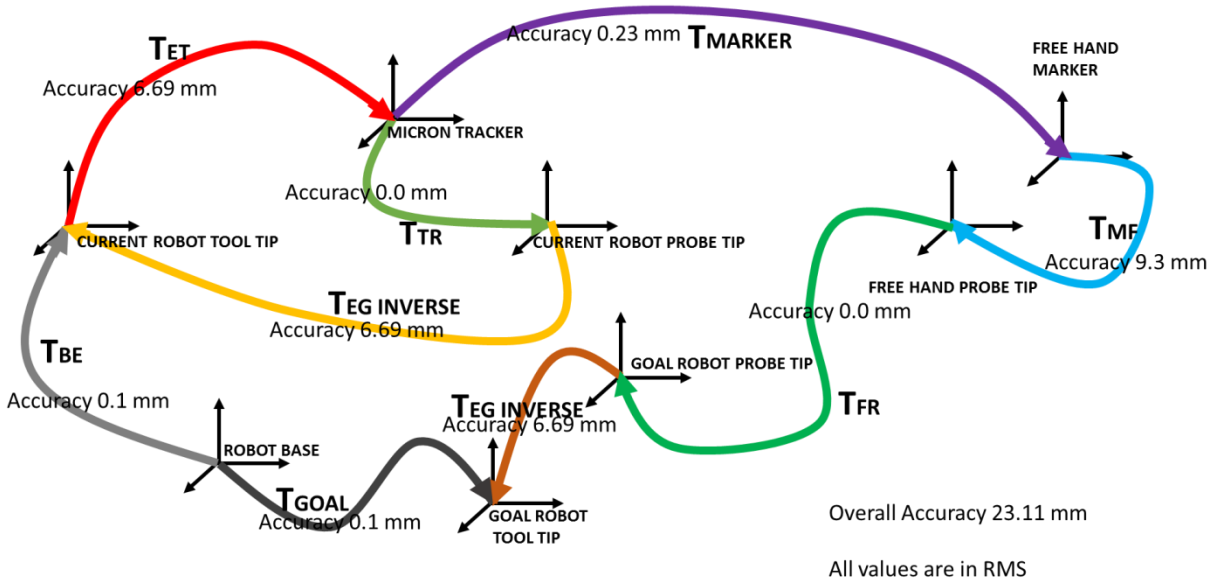


**Figure 34. Theoretical Accuracy Calculation**

The overall accuracy is the sum of the rms values of accuracy of various components of the transformation above and they turn out to be 23.11 mm rms.

The best way of finding the accuracy is to have a different tracking system which always tracks known markers on the free hand probe and the robot ultrasound probe to find the difference between their actual positions to get the accuracy of the entire system which will be done as future work.

## *3.10 EPT experiment*

In order to show the feasibility of the energy profile tracking (EPT), an experiment was conducted in which the ultrasound probe connected to an ultrasound machine sends ultrasound waves through a thin layer of rubber and then through the water; a hydrophone is put inside the water at a distance of about 7 cm. The hydrophone is connected to an oscilloscope to monitor the received signal. Figure 35 shows the ultrasound machine settings in this experiment while Figure 36 shows the experiment setup.

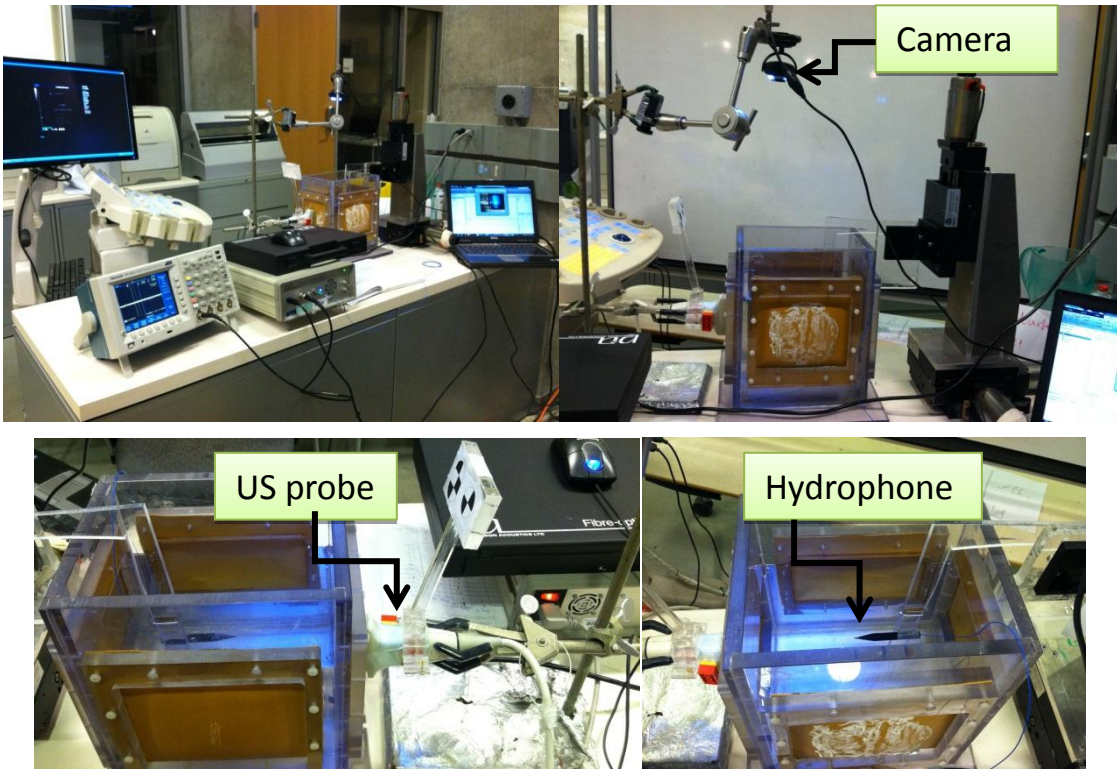


**Figure 35. EPT experiment setup**

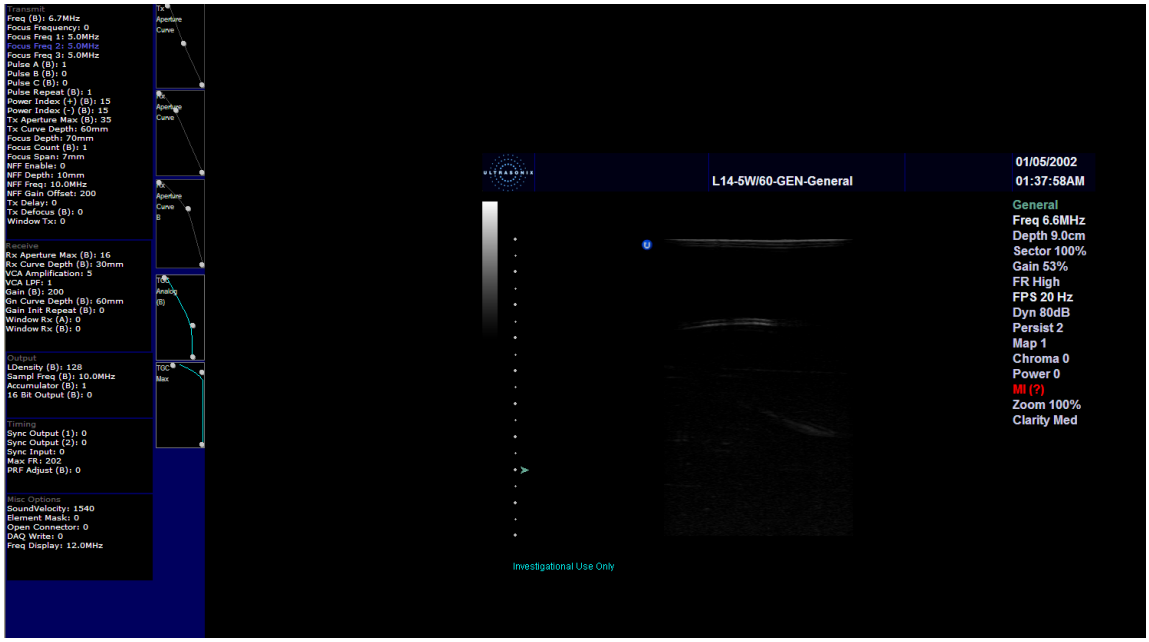


**Figure 36. Ultrasound settings for EPT experiment**

We found the position where we could get the maximum peak-peak signal strength along z-axis of ultrasound image and labeled that as 0. Then we used microstage to move the hydrophone half a millimeter by half a millimeter to the right and then to the left till 4 mm. At each step, we waited for a few seconds and recorded the maximum observed peak-to-peak voltage. At the same time a picture of the hydrophone and probe was taken using the camera. Table shows the results of this experiment.

**Table 2. EPT experiment results**

| Z (along probe)(mm) | Max pick-pick observed in a few seconds in hydrophone(mv) |
|---|---|
| **-4.0** | 5.11 |
| **-3.5** | 5.89 |
| **-3.0** | 6.16 |
| **-2.5** | 6.46 |
| **-2.0** | 6.69 |
| **-1.5** | 6.99 |
| **-1.0** | 7.11 |
| **-0.5** | 7.61 |
| **0.0** | 7.68 |
| **0.5** | 5.53 |
| **1.0** | 5.70 |
| **1.5** | 5.73 |
| **2.0** | 5.03 |
| **2.5** | 4.92 |
| **3.0** | 4.30 |
| **3.5** | 4.09 |
| **4.0** | 3.81 |

Figure 37 shows a plot of data shown in Table 2.

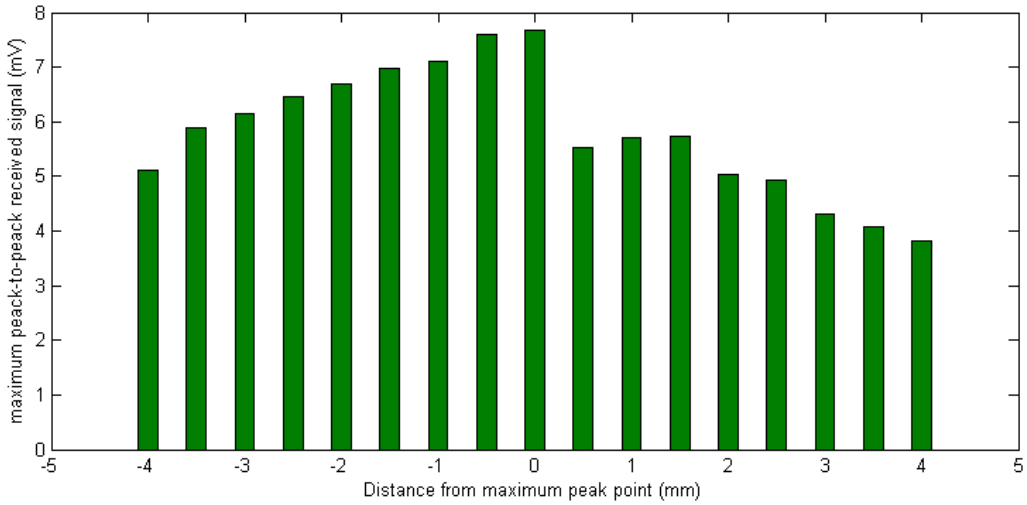


**Figure 37. plot of EPT recorded data**

It can be seen that, in general, the more distance from the point labeled as zero, the less peak-peak signal strength is observed. Figure 38 shows the pictures taken for the 0, 1, 4, and -4 mm points. It can be seen that when the hydrophone is at point 0, it is visually aligned with the probe.

A demo video of this experiment is available at [12]. In the video, top right window shows the top view of hydrophone (in water) and ultrasound probe outside the water tank. Top left window shows the oscilloscope showing the signal strength received by hydrophone. Bottom left shows the microstage used to move the hydrophone. Each turn is equivalent to 1 mm. The video shows how the average peak increases when the hydrophone gets aligned with the probe and decreases when it gets far from the alignment.

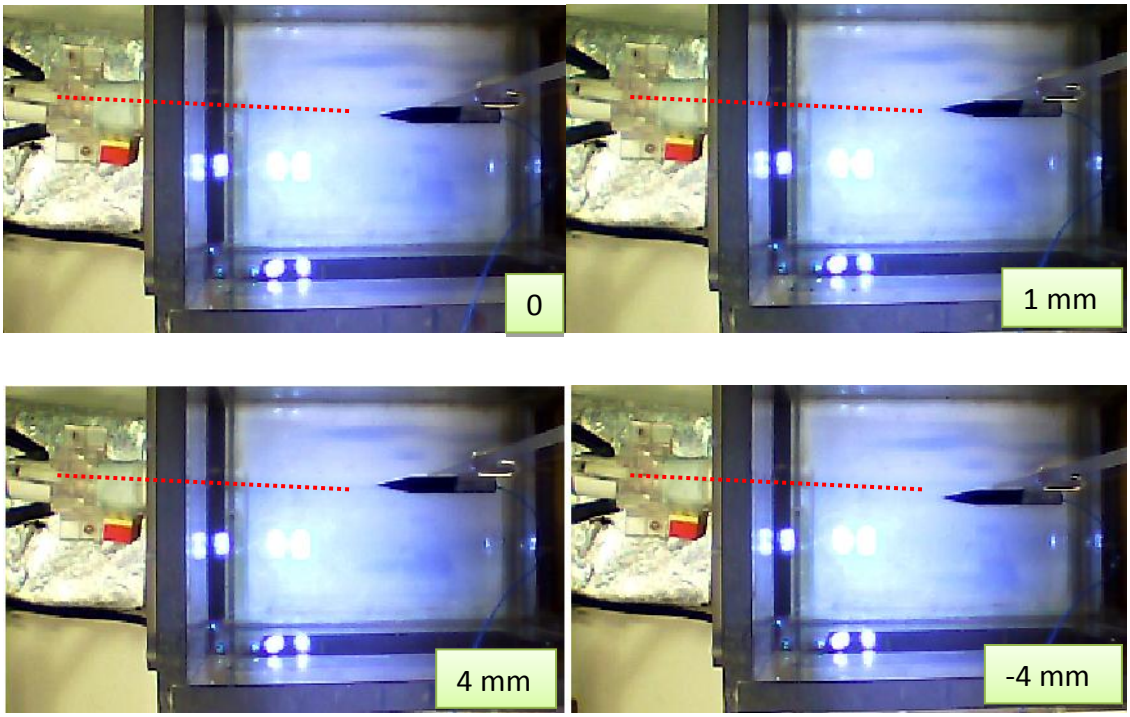


**Figure 38. EPT experiment top view pictures**

# 4 Conclusion and future work

In this project, a robot assisted ultrasound system is developed in which a robot operated probe is capable of following the position of a freehand probe. This system can be used for high penetration ultrasound imaging for obese patients, fast scanning, or soft tissue ultrasound tomography. The system can benefit from three loops of tracking: tracker, B-mode, and EPT. The first two tracking loops are implemented and the EPT feasibility is studied through and experiment. A hand-eye calibration and two ultrasound calibrations are done and the accuracy evaluations are provided.

In the next step, the robotic mock probe should be replaced with real ones. The accuracy of the system can be improved by more accurate calibrations and implementation of EPT alignment. The rotation tracking is implemented but should be tested and be improved. In addition, a more appropriate robot with a larger workspace and 6 DOF should be used. The endeffector design can be improved to have a stronger rigidity. After the system's accuracy is tested and improved to sub-millimeter, reconstruction algorithms can be utilized to produce soft tissue tomographic images.

# 5 Management summary

In our first project plan, we did not consider some major tasks including calibrations and several mechanical designs. Throughout the project we learnt to divide the project into more detailed steps and be more specific in the tasks; hence we proposed a new project plan. We encountered several unresolved dependencies but we learnt to have backup plans that can replace the missing part and match other parts of the project in a timely manner. Should we have more time, we would improve the system accuracy and perform more extensive system evaluations.

We tried to cooperate in most parts of the project to learn the most but initially we assigned responsibilities to each of us. Fereshteh was responsible for incorporation of the tracking system, probe holders and endeffector design, and ultrasound calibration while Rishabh was responsible for mock probes design, incorporation of robot, code development, and hand-eye calibration.

We delivered minimum, expected and part of the maximum deliverables presented in our second checkpoint presentation:

- ultrasound calibrated probes and hand-eye calibrated endeffector,
- a robot operated mock ultrasound probe following the position of a free hand ultrasound probe using optical tracking system combined with B-mode tracking,
- an experiment showing feasibility of Energy Profile Tracking (EPT), and
- evaluation study of calibrations.

The remaining part from maximum deliverables is:

- Real images shall be collected and reconstructed on a PC to display real-time ultrasound images.

In comparison with deliverables planned in project plan, we combined tracking system alignment with B-mode alignment, and eliminated building of transparent phantom as it was not needed.

# 6 Acknowledgement

We would like to thank our mentors Professors Taylor, Boctor, and Iordachita for their great support and guidance. We would also like to thank Professor Kazanzides, Min Yang, Reza Seifabadi, Xiaoyu Guo, Alexis Cheng, Bark Gonenc, Dr. Pezhman Foroughi, Professor Ziv Yaniv, and Hyun-Jae Kang for their help throughout this project.

# 7 References

[1] http://en.wikipedia.org/wiki/Medical_ultrasonography, accessed: 5/10/2013 10:55 AM

[2] Schomberg, H. "An improved approach to reconstructive ultrasound tomography,"J Phys D

Appl Phys 1978;11:L181–5.

[3] http://www.diffen.com/difference/CT_Scan_vs_Ultrasound, accessed: 5/10/2013 11:16 AM

[4] http://www.dimensionsinfo.com/how-big-is-a-ct-scanner/, accessed: 5/10/2013 11:16 AM

[5] http://www.absolutemed.com/Medical-Equipment/Ultrasound-Machines/GE-Vivid-e-

Portable-Ultrasound-Machine, accessed: 5/10/2013 11:17 AM

[6] MicronTracker Developer manual available in the MicronTracker shipped package

[7] L. Mercier, T. Lango, F. Lindseth, L. Collins, “A Review of Calibration Techniques for Freehand 3D Ultrasound Systems,” Ultrasound Me. & Biol., Elsevier, Vol. 31, No. 2, pp. 143-165, 2005.

[8] Diane M. Muratore, Robert L. Galloway Jr, "Beam calibration without a phantom for creating a 3-D freehand ultrasound system," Ultrasound in Medicine & Biology, Volume 27, Issue 11, November 2001, Pages 1557-1566.

[9] Khamene A, Sauer F., "A novel phantom-less spatial and temporal ultrasound calibration method," Med Image Comput Comput Assist Interv., Volume 3750, 2005, Pages 65-72.

[10] Z. Yaniv, P. Foroughi, H. J. Kang, E. Boctor, "Ultrasound calibration framework for the image-guided surgery toolkit (IGSTK)," Proc. SPIE 7964, Medical Imaging, March 2011.

[11] http://mason.gmu.edu/~potto/matlab/uread.m, Apr. 21, 10:40 AM

[12] http://www.youtube.com/watch?v=z9_ahzlt0tI

# 8 Appendix

Project package uploaded on website contains the following items:

- US_calibration: US calibration tracker data and codes for analysis and verification
- US_data: US images and feature extraction codes
- Markers: markers used for pointer and freehand probe
- Solidworks: final mock probe design, marker and camera placement simulation files, endeffector design files, marker holders files
- Ept: Pictures and waveforms, oabserved data, and video for EPT experiment
- Robot codes, hand-eye calibration accuracy calculation code